Dielectric Properties of Vacuum Evaporated SnS Thin Films

Bushra A. Hasan

University of Baghdad, College of science, Physics Department, Baghdad, Iraq.
Email: bushra_abhasan@yahoo.com

Abstract: Tin Sulfide SnS thin films with different thicknesses (t=100, 200, and 300nm) were synthesized successfully by thermal evaporation process. The dielectric permittivity ε and ac conductivity σ_{ac} were measured at temperatures in the range of 293–493 K and frequencies in the range of 10 kHz–100MHz. It is found that there are two conductivity mechanisms and hence two activation energies converts to one mechanism with the increase of t. The ac activation energy E_{AC} decreases with thickness and frequency. The exponent *s* shows a progressive decrease with *t*. The results are explained in terms of structural difference by the effect of *t* and thermal treatment. Few anomalies in dielectric studies were observed near 340 and440K, respectively. These points were related to crystalline phase transitions.

Keywords: SnS semiconductor, thermal evaporation, dielectric properties

1. Introduction

In recent years, thin films of SnS have attracted much attention for the photovoltaic applications due to the high absorption coefficient ($\approx 10^4 cm^{-1}$ near the fundamental edge) [1,2] and high conductivity (hole mobility = 90 $cm^2 V^{-1} s^{-1}$). SnS belongs to groups IV-VI of compounds formed with Sn as the cation and S as the anion. The constituent elements are inexpensive, nontoxic and abundant in nature leading to the development of devices that are environmentally safe and have public acceptability. SnS is an important optoelectronic material that is found in zinc blend with the lattice constant (*a* =0.5845 nm) [3], orthorhombic with the lattice constants (*a* =0.385 nm, *b* =1.142 nm and *c* =0.438 nm) [4,5] and herzenbergite [6] crystal structures. SnS shows a p-type electrical conductivity and its electrical conductivity can be controlled by using different dopants like Al, Ag and Cl. The optical properties of SnS vary depending on the synthesizing or fabrication method, but most work agrees with direct (1.2-1.5 eV) and indirect (1.0-1.2 eV) band gap values. These properties enable SnS thin films to be used as an absorption layer in the fabrication of heterojunction solar cell [4,7]. SnS thin films can be generated by many methods such as thermal evaporation [8], pulse electrode position [9], spray pyrolysis [10], SILAR [11], electron beam evaporation [12], chemical bath deposition [13]. The film in this study is grown by chemical bath deposition (CBD) which creates a thin film on a solid substrate via a reaction in a liquid solution. The CBD method is inexpensive, easy to prepare and its necessary vessels can be found in an ordinary chemistry laboratory. Therefore, this method has many advantages over others used to

grow semiconductor thin films. In this work, we report on the A.C properties of SnS thin films by thermal deposition under vacuum. Moreover, we present the activation energy value from the temperature-dependent conductivity measurement. An analysis of the published data indicates that little is known about the a.c conductivity of SnS thin films. Because of this reason, an attempt has been made to deposit SnS thin films with different thicknesses at room temperature in the present work. SnS that have been carried out till date, the experimental results on dielectric study are very few, and that too are very less informative . It is well known that dielectric properties of every solid are very sensitive to the local electric field distribution in the sample. Therefore, the temperature and frequency dependence of dielectric constant and loss can explore useful information about structure changes, transport mechanism and defect behavior.

2. Experimental Description

Source material, SnS was prepared by melting high purity elements (99.99%) Sn and S in an evacuated quartz tube at a temperature of 1173 K. Tin sulfide films with different thicknesses (100,200,and 300nm)were deposited on corning 7059 microscopic glass substrate by thermal evaporation technique under high vacuum (10^{-5} Torr) at room temperature. The distance between source and substrates, rate of deposition have been maintained as constant at 15 cm and 8 Å/s, respectively**.** The as-deposited thin films of SnS were characterized for structural, and dielectric properties. The composition of the films was estimated using atomic absorption spectroscopy (AAS). Optical Interference Fringes was used to measure film thickness and Fizaeu fringes of equal thickness are obtained in an optical apparatus of the type ,the film thickness (d) is given by:

$$d = \frac{\lambda}{2} \frac{\Delta x}{x} \tag{1}$$

Where Δx is the shift between interference fringes. λ is the (Na) wavelength (589.3nm) and x is the distance between interference fringes. The samples having almost thickness of about $t \pm 10nm$.

The phase of the synthesized thin films was confirmed by X-ray diffraction analysis. Further, the crystallite size was calculated by Scherer formula and found to increase from 58 to 79 nm with increase of thickness. For thickness, t=300nm, the films showed orthorhombic OR phase with a strong (111) preferred orientation. The films deposited with thickness < 200nm deviated from stoichiometry and additional phases such as Sn_2S_3 was found to be present. The prepared thin films were then used for dielectric measurement by coated its opposite faces using high grade conducting layer of Silver paste. The variation of dielectric constant (real and imaginary), loss and ac conductivity with temperature at different frequency (10k Hz-10MHz) was studied from room temperature to 220 ^{o}C using Hewlett Packard model (HP4274A & HP4275A).The results were analyzed and discussed in detail.

3. Results and Discussion

3. 1 A. C Conductivity

The ac conductivity can be directly related to the imaginary part of deictic constant ε_i as $\sigma_{ac} = \omega\varepsilon_0\varepsilon_i$ where ε_0 and ω are the permittivity of free space and angular frequency respectively. The variation of ac conductivity with frequency and temperatures (293-493K) of SnS of different thicknesses is shown in Fig.1. A smooth increase in the ac conductivity is observed throughout the temperature for lower thicknesses, while σ_{ac} decreases with temperature for higher thicknesses. The ac conductivity patterns for lower thickness show a frequency independent plateau in the low frequency region and exhibits dispersion at higher frequencies. This behavior obeys the universal power law [31,32], $\sigma(\omega) = \sigma_0 + A\omega^s$ where σ_0 is the dc conductivity (frequency independent plateau in the low frequency region), A is the pre-exponential factor and s is the fractional exponent between 0 and 1.The conductivity spectrum for t=100nm is frequency dependent in the hole frequency range where the deviation from σ_{dc} (plateau region) is more prominent .The increase of thickness the conductivity spectrum differs such that frequency independent plateau expand to high frequency range specially at t= 300nm , however the increase of temperature adminished   the independent frequency plateau region . The deviation from σ_{dc} (plateau region) value in the conductivity spectrum (in the low frequency region) is due to the electrode polarization effect. The values of n were obtained by fitting the $\sigma(\omega) = \sigma_0 + A\omega^n$, s is tabulated in Table1. Generally, power law exponents (s) exceeded unity for t=100 and 200nm. It is found that s value decreases with the increase of thickness indicating the ideal long-range pathways and diffusion limited hopping (tortuous pathway) respectively [33].The value of exponent of the higher frequency slopes (Table-1) shows that the long-range drift of charge carriers may be one of the sources of conduction. From the Table-1, it is clear that the dc conductivity (σ_0) increases with increase in thickness. It is clear that *s value* for t=300nm are less than unity which confirmed the hopping mechanism [34]. It is obvious that s decreases with temperature for lower thicknesses (100,200nm) which makes the correlated barrier hopping (CBH) the most suitable model. The CBH model is adopted when the electrons hop over the potential barrier between two sites; the ac conductivity is due to hopping between defect states or dangling bonds (D^+D^-). In CBH, the $\sigma_{ac}(\omega)$ is exponentially dependent on temperature, while s for t= 300nm decreases with t in the first stage and then increases with increase of *T*; hence small poloran (SP)is the suitable model. When the exponent *s* gets to rise with the increase of temperature for high thicknesses (300nm), this occurs when the addition of the charge carrier to the covalent solid causes a large degree of local lattice distortion, which forms a small polaron [35].

The activation energy for conduction (E_{ac}) in the entire region as shown in figure .2. The values of ac activation energy (E_{ac}) for SnS films were determined from the plot of Ln $\sigma_{ac}(\omega)$ against the reciprocal of Kelvin temperature. E_{ac} were estimated by fitting different regions with the Arrhenius equation $\sigma_{ac} = \sigma_o \exp-\dfrac{E_a}{kT}$ [36] and is illustrated in table 2 at selected frequencies (10 kHz, 100 kHz, and1MHz). The data show that each sample reveals two conduction mechanisms. Moreover,

the values of E_{ac} decrease with increasing frequency, while the same decreases with thickness. For example, E_{ac} decreases from 0.153 to 0.0193 eV when the frequency increases from 10k Hz to 100 kHz and while E_{ac} decreases from 0.153 to 0.094 eV when t increases from 100 to 300nm. The decrease of E_{ac} with the increase of frequency results from the increase of vibrating energy supplied from the increasing frequency of the electric field which causes the decrease of E_{ac} values. This affirms the conductivity is pure ac. The decreases of E_{ac} can be explained as the action of increase grain size .

Fig.3 and 4 show that the variations of ε_r, with frequency for the SnS films having different thickness and at different temperatures respectively. In all the cases, a strong frequency dispersion of permittivity is observed at low frequency region followed by a nearly frequency independent behavior above100 kHz and 10MHz for t=100 and200 ,300 respectively . The decrease of (ε_r) with increase in frequency may be attributed to the electrical relaxation processes, but at the same time the material electrode polarization cannot be ignored. The material electrode interface polarization superimposed with other relaxation processes at low frequencies. It is seen that with increase of thickness, (ε_r) value increases in the lower frequency and nearly same in the higher frequency region. The thickness increment may result in more localization of charge carriers along with mobile ions causing higher conductivity. This may be the reason for higher (ε_r) and strong low frequency dispersion.

On the other hand the real dielectric constant increases with temperature up 443K but then decreases with further increase of temperature. Indeed ε_r increases from0.0997to 0.108when thickness increases from 100 to 300nm.

The temperature dependence of real dielectric constant ε_r at different fixed frequencies over the temperature range of 293-493 K of SnS films with different thickness is shown in Fig. 4. A broad dielectric peak near 450K and 340K for thickness 100, 200 and 300nm respectively is attributed to the phase transition temperature from zinc blend to orthorhombic structure [37].It is obvious that the transition temperature decreases with the increase of thickness.

Is it useful to distinguish long-range conduction process from the localized dielectric relaxation. To visualize this, we have plotted the imaginary part of complex dielectric permittivity ε_i as a function of frequency for SnS films with different thicknesses as representatives Fig. 5. Dielectric relaxation is a result of the reorientation process of dipoles, which show a peak in ε_i spectra. For SnS samples with higher ion concentration, the movement of ions from one site to another will perturb the electric potential of the surroundings. Motion of the other ions in this region will be affected by perturb potential. Such a cooperative motion of ions will lead to non-exponential decay, or a conduction processes with distribution of relaxation time [38]. It has been observed that (Figure 5) in the imaginary part of dielectric spectra, a relaxation peak is observed for the ε_i for lower thickness i.e. t=100nm , whereas no well pronounce peak is observed in the dielectric spectra for higher thicknesses. This suggests that charge motion strongly coupled manifesting as a single

peak in the ε_i spectra with no corresponding feature in dielectric spectra for higher thicknesses [39]. So the conduction takes place through charge migration of ions between coordinated sites of along with the segmental relaxation of semiconductor. An enhanced of conduction is a natural consequence of thickness increment. The higher value of dielectric loss ε_i at low frequency is due to the free charge motion within the materials. On thickness increment ε_i increases in the lower frequency region reflect the enhancement of mobility of charge carrier. As the temperature increases ε_i first decreases with rise in frequency in low frequency region followed by a peak in the loss spectra. The loss peak for lower thickness is shifting towards the higher frequency side with the increase of temperature while loss peak is shifting towards the lower frequency side with the increase of temperature for higher thicknesses. The appearance of peak is attributed to the relaxation phenomena. Similar types of observations have been reported in literature [40,41]. It is generally believed that dielectric data is characterized by superposition of two processes: conductivity contribution that produces an increase of both real part ε_r and the imaginary part ε_i of the dielectric function on decreasing frequency and a relaxation process exhibiting a maximum in ε_i that shifts higher frequency side with increase in temperature. The measured dielectric loss ε_i spectrum contains contribution from two sources: dipolar orientation and diffusion of charge carrier. When interfacial polarization occurs thickness resulted in overall increase of ε_i and ε_i due to free charge contributions. So the increase of the molecular mobility is reflected both by increase of free charge mobility and the shift of the peak towards the higher frequency side with simultaneous increase of its magnitude (Fig. 5). The over all result is enhancement of conductivity on thickness increment.

A direct evidence of the existence of multi-relaxation time in the as-deposited SnS films treated at temperature in the range from 293 to 493 K is obtained by plotting Cole–Cole diagrams as shown in Figure 6. It has been observed that as thickness increases, ε_r versus ε_i curves represent the arc of circles having their centers lying below the abscissa axis will be vanished. This confirms the existence of the distribution of τ in for lower thickness films. By measuring the angles ($\alpha\pi/2$) the values of the polarizability (α) have been determined and were listed in table 1. We can note that the values of α declares a non systematic variation with the increase of thickness and thermal treatment temperature. However, in general α tends to increase with thermal treatment temperature. This is in agreement with the concept of molecular relaxation; the increase of α value results from the reduction of the forces as a result of the formation of the barrier between elements, while the decrease of α with the increase of heat treatment results from the rise of the forces of the intermolecular, i.e. α increases from 0.133 to 0.277 when T increases from 293 to 343 K while α decreases from 0.222 to 0.055 when the temperature of thermal treatment T increases from 443 to 493 K for samples with thickness 100nm [42,43].

Table.1 Illustrates the values of s and α of SnS films**.**

Thickness(nm)	Oven Temperature (K)	s	α
100	293	1.055	0.133
	343	1.34	0.277
	393	1.121	0.166
	443	1.028	0.222
	493	0.9757	0.055
200	293	1.055	-
	343	1.34	-
	393	0.838	-
	443	0.6654	-
	493	0.2951	0.444
300	293	0.6229	-
	343	0.3436	0.222
	393	0.2072	-
	443	0.9879	0.1
	493	0.7142	0.244

Table 2. Illustrates the E_{ac} values of SnS films.

Thickness (nm)	F=10kHz		F=100kHz	F=1000kHz
	E_{ac1}(eV)	E_{ac2}(eV)	E_{ac1}(eV)	E_{ac1}(eV)
100	0.153	0.0637	0.0458	0.0193
200	0.146	0.0578	0.0442	0.0177
300	0.094	0.0445	0.0428	0.0164
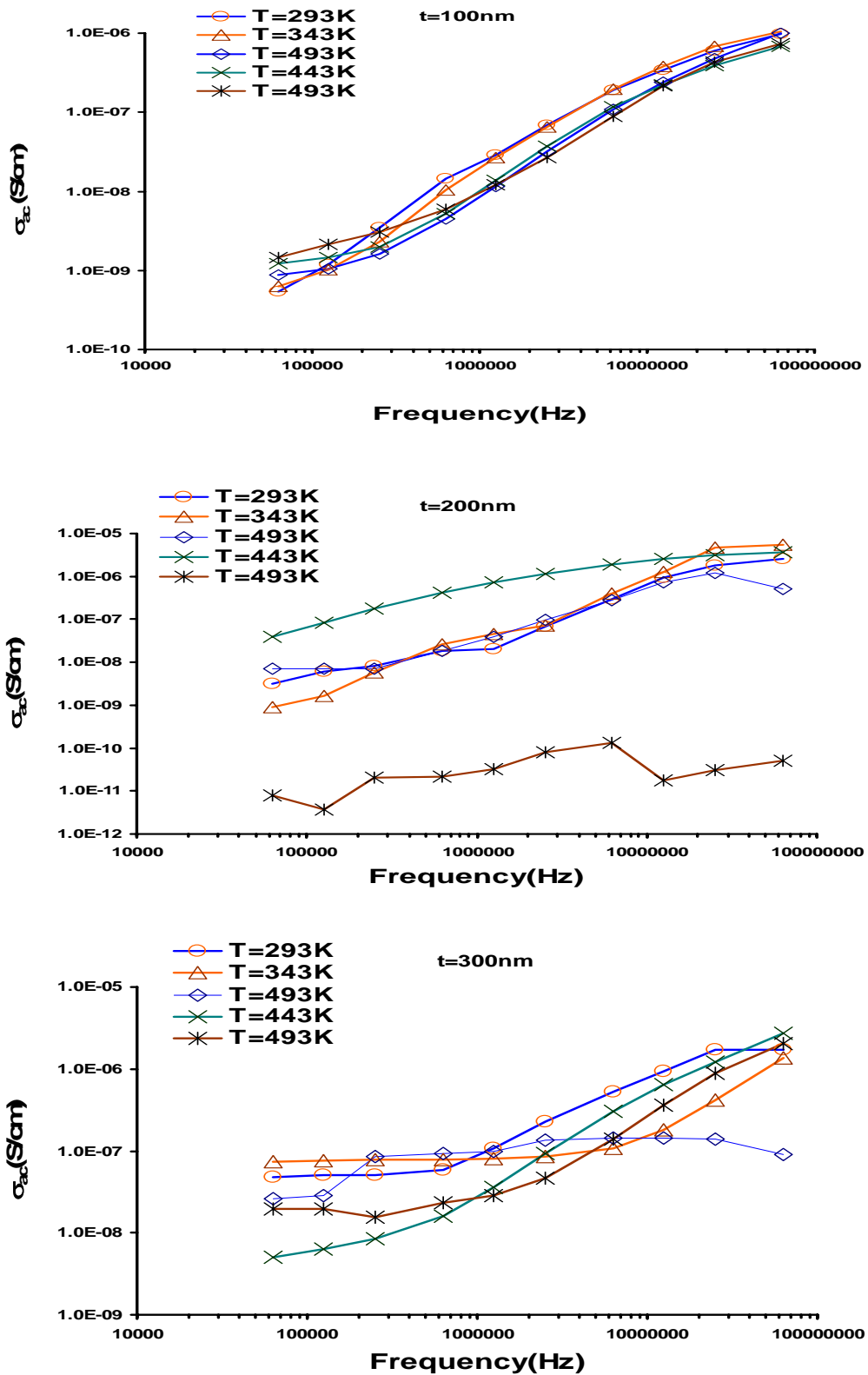
Fig. 1. Frequency dependence of AC conductivity for SnS film with different thicknesses and temperatures.
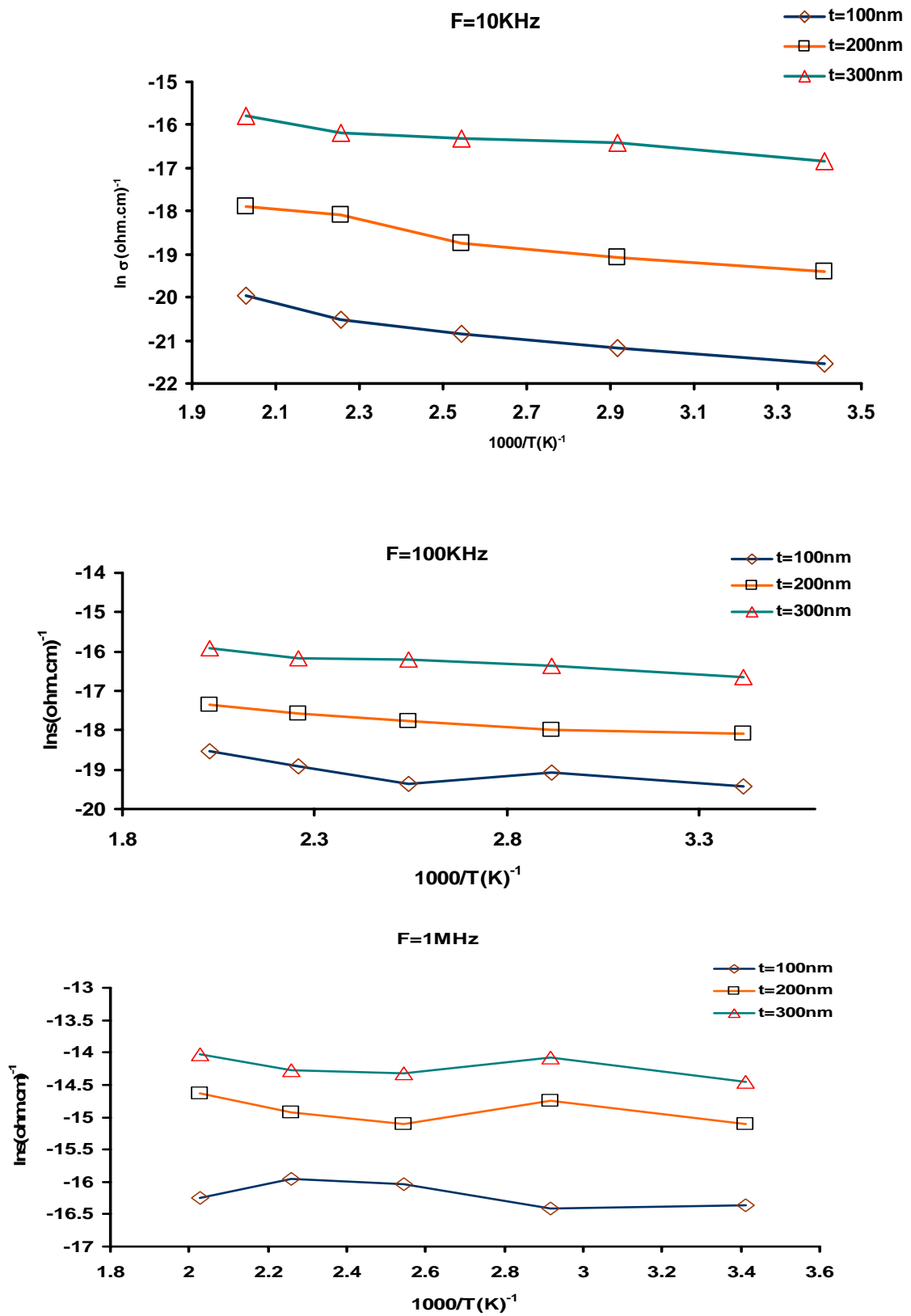
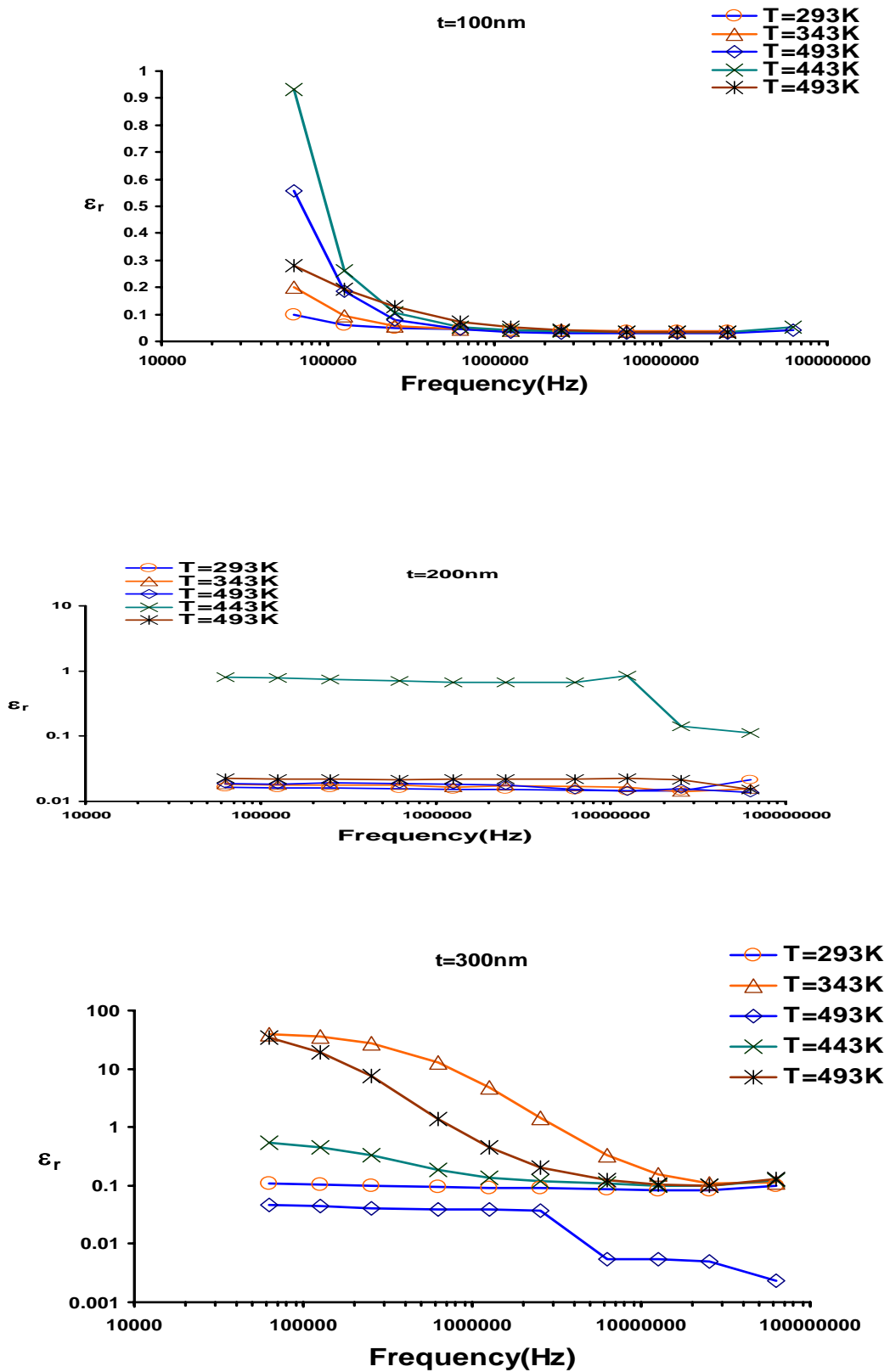**Fig. 2.** Plot of ln ac conductivity versus 1000/T characteristics for a film of thickness 100 nm.

Fig. 3. Variation of real part of permittivity (ε_r) with frequency of SnS films with different thicknesses and temperatures
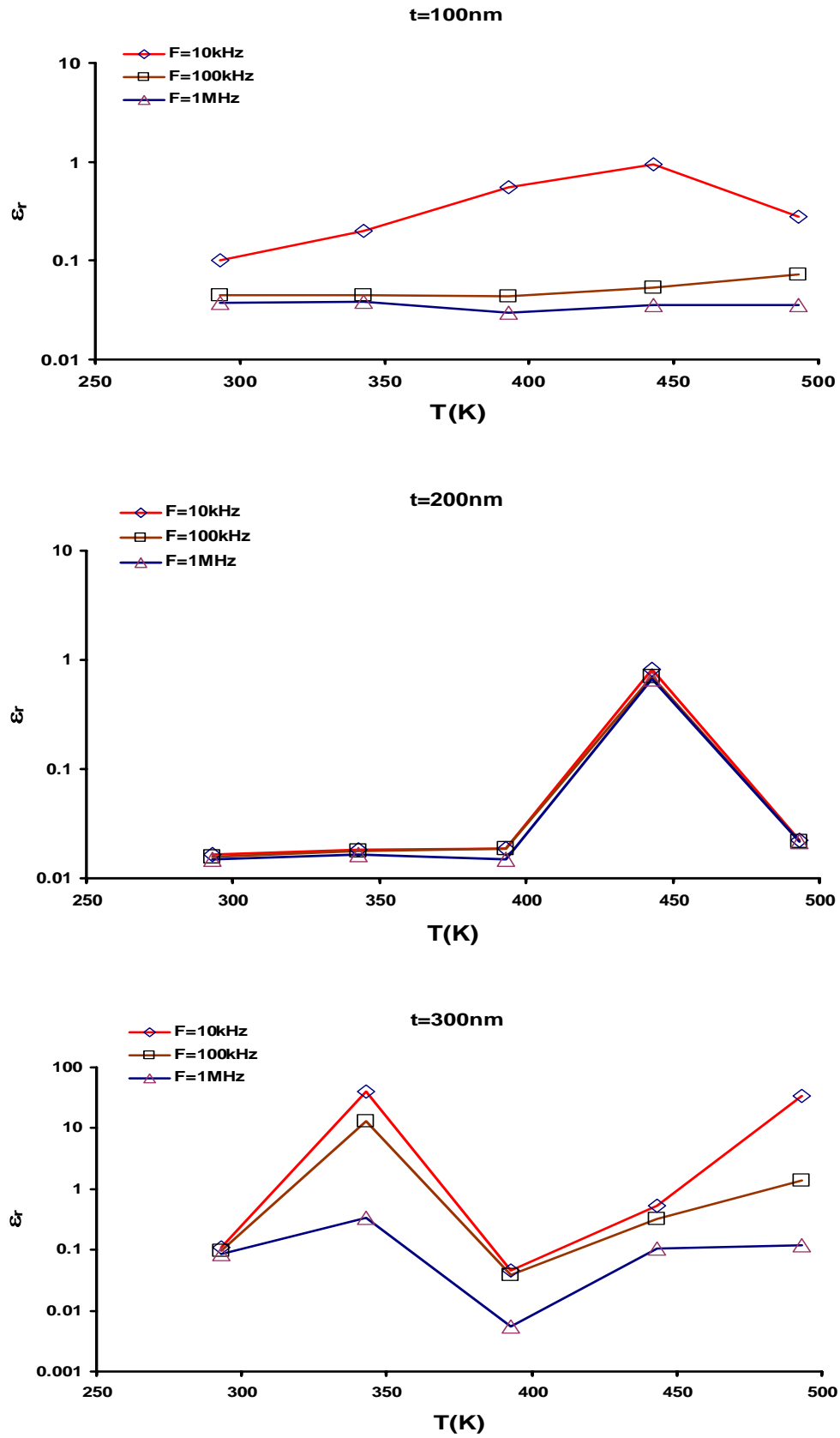
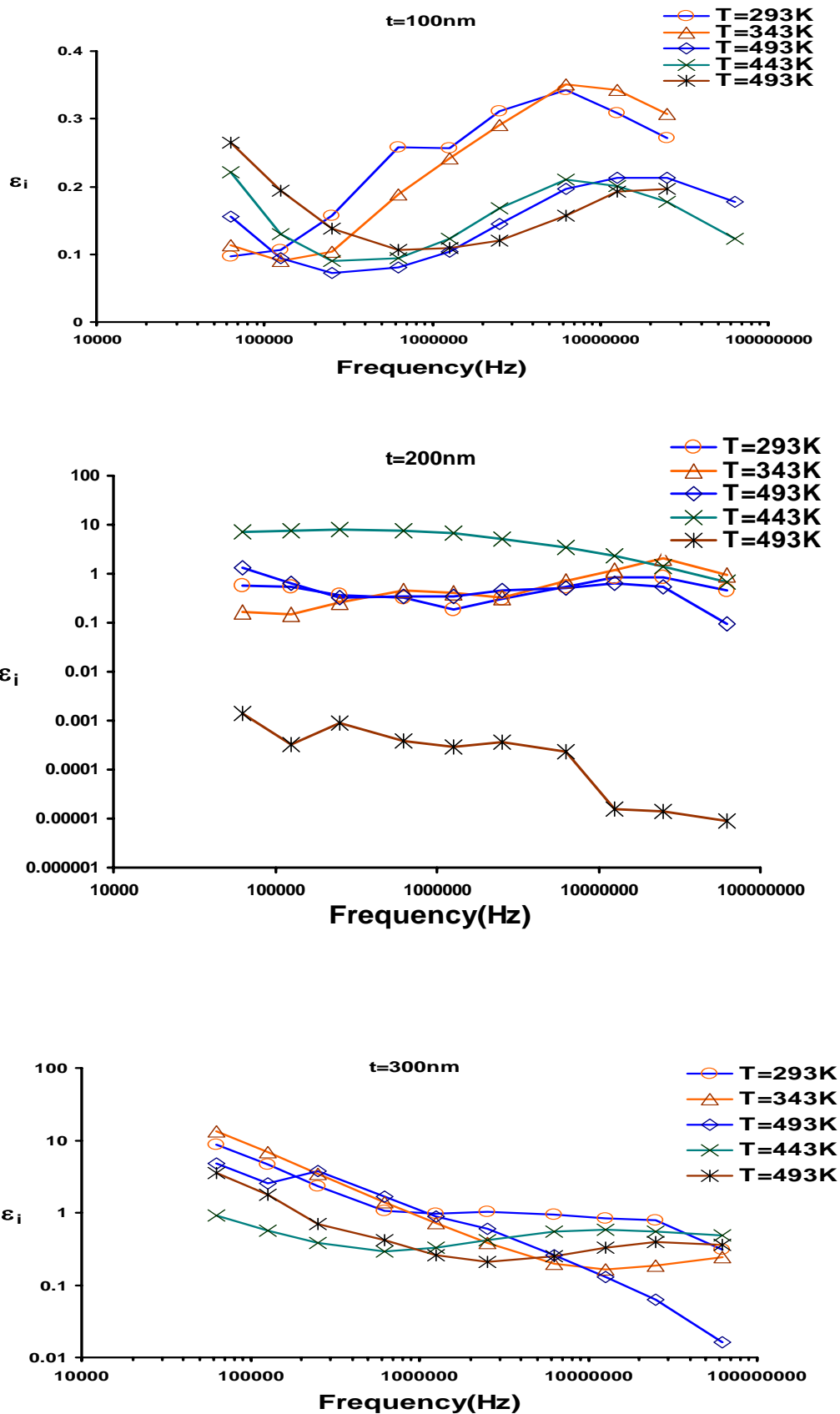**Fig. 4.** Temperature dependence real part of permittivity (ε_r) for SnS film with different thicknesses at 10 kHz

Fig. 5. Variation of imaginary part of permittivity (ε_i) with frequency of SnS films with different thicknesses and temperatures.
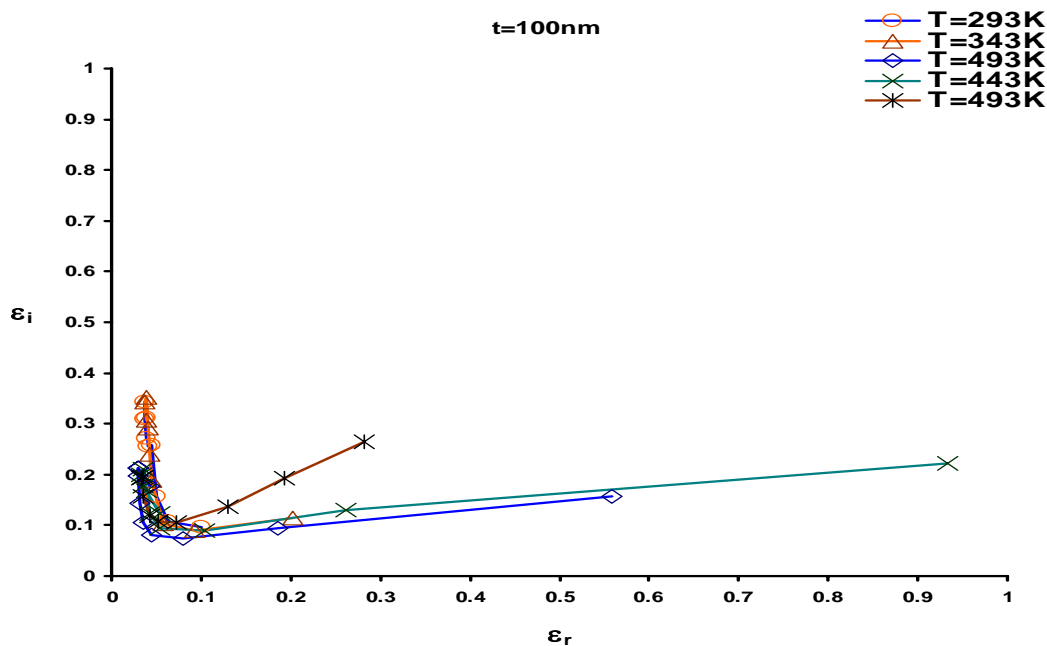
Fig. 6. Cole – Cole diagrams of SnS films for different temperatures.

4. Conclusions

From this work, the following prints may be concluded:

1. Slope values (s) of SnS films show progressive decrease with thickness.

2-The conductivity is pure ac for lower thickness, while the conductivity is frequency independent for high thickness.

3. The increase of SnS thickness causes the proceeding reduction of s, i.e. increases the d.c conductivity .

4. The increase of thickness leads to reduces the values of polarisability of SnS films consequently increases the intermolecular force ,while increase of temperature reduces the force of the intermolecular through out formation a barrier.

Acknowledgments

References

[1] E. C. Greyson, J. E. Barton, T. W. Odom, Small, **2**, 368–371 (2006).

[2] J. B. Johnson, H. Jones, B. S. Latham, J. D. Parker, R. D. Engelken, C. Barber, Semicond.Sci. Technol., **14,** 501-507 (1999).

[3] A. Akkari, C. Guasch, N. Kamoun-Turki, J. Alloy Compd., **490,** 180–183 (2010).

[4] S. Cheng, Y. Chen, C. Huang, G. Chen, Thin Solid Films, **500,** 96–100 (2006).

[5] M. Devika, N. Reedy, K. Ramesh, K. Gunasekhar, E. Gopal, K. Reddy, Semicond. Sci.Technol., **21,** 1125-1131 (2006).

[6] D. Avellaneda, G. Delgado, M. Nair, P. Nair, Thin Solid Films, **515,** 5771–5776 (2007).

[7] N. Sato, M. Ichimura, E. Araia, Y. Yamazaki, Sol. Energy Mater. Sol. Cells, **85,** 153 (2005).

[8] O. E. Ogah, G. Zoppi, I. Forbes, R. W. Miles, Thin Solid Films, **517,** 2485 (2009).

[9] G. H. Yue, W. Wang, L. S.Wang, X. Wang, P. X. Yan, Y. Chen, D. L. Peng, J. Alloy Compd. , **474,** 445 (2009).

[10] E. Guneri, C. Gumus, F. Mansur, F. Kirmizigul, Optoelectron. Adv. Mat., **3,** 383 (2009).

[11] B. Ghosh, M. Das, P. Banerjee, S. Das, Appl. Surf. Sci., **254,** 6436 (2008).

[12] A. Tanusevski, D. Poelman, Sol. Energy Mater. Sol. Cells, **80,** 297 (2003).

[13] M. T. S. Nair, P. K. Nair, Semicond. Sci. Technol., **6,** 132 (1991).

[14] N. K. Reddy, K. T. Ramakrishna Reddy, Thin Solid Films, **325,** 4 (1998).

[15] G. Hodes, Chemical solution deposition of semiconductor films, Merker Dekker, Inc., New York, 31-131 (2003).

[16] P. P. Hankare, A. V. Jadhav, P. A. Chate, K. C. Rathod, P. A. Chavan, S. A. Ingole, J. Alloy Compd., **463,** 581 (2008).

[17] M. M. El-Nahass, H. M. Zeyada, M. S. Aziz, N. A. El-Ghamaz, Opt. Mater., **20,** 159 (2002).

[18] B. Thangaraju and P. Kaliannan, J. Phys. D: Appl. Phys., **33,** 1054 (2000).

[19] M. Mnari, N. Kamoun, J. Bonnet, M. Dachraoui, C. R. Chimie, **12,** 824 (2009).

[20] P. Pramanik, P. K. Basu, S. Biswas, Thin Solid Films, **150,** 269 (1987).

[21] B. Cullity, Elements of X-ray diffraction, Addision-Wesley Publishing Company Inc., USA, **501** (1967).

[22] G. Willeke, R. Dasbach, B. Sailer, E. Bucher, Thin Solid Films, **213,** 271 (1992) .

[23] G. B. Williamson, R. C. Smallman, Philos. Mag., **1,** 34 -46 (1956).

[24] J. Garnier, A. Bouteville, J. Hamilton, M. Pemble, I. Povey, Thin Solid Films, **518,** 1129 (2009).

[25] S. Lopez, A. Ortiz, Semicond. Sci. Technol., **9,** 2130 (1994).

[26] M. M. Nassary, temperature dependence of the electrical conductivity, J. Alloy Compd., **39,** 21 (2005).

[27] S. Kasap, P. Capper, Handbook of electronic and photonic materials, Springer Science+Business Media, Inc., 47-74 (2006).

[28] N. K. Reddy, V. Reddy, P. Datta, R. Miles, Thin Solid Films, **403–404,** 116 (2002).

[29] A. Tanusevski, Semicond. Sci. Technol., **18,** 501 (2003).

[30] K. Deraman, S. Sakrani, B. Ismail, SPIE, **2364,** 357 (1994

[31] A. K. Jonscher, *Dielectric Relaxation in Solids*, Chelsea Dielectric Press, London, (1983).

[32] A. K. Jonscher, *Nature,* **267**, 673 (1977).

[33] K. A. Mauritz, *Macromolecules,* **22**, 4483 (1989).

[34] K. P. Singh and P. N. Gupta, *European Polymer Journal,* **34**, 1023 (1998).

[35] S. Ramesh, A. H. Yahaya and A. K. Arof , *Solid State Ionics,* **291**, 152-153 (2002).

[36] B. Natesan, N. K. Karan and R. S. Katiyar, *Phys. Rev., E* **74** 042801 (2006).

[37] David Avellaneda, M.T.S. Nair, P.K. Nair, Thin Solid Films, **517,** 2500–2502 (2009).

[38] Y. Fu, K. Pathmanathan and J. R. Steven, *J. Chem. Phys.,* **94,** 6326 (1991).

[39] P. Jeevanandam and S. Vasudevan, *J. Chem. Phys.*, **109**, 8109 (1998).

[40] F. Kremer and A. Schonhals (Eds.), *Broad Band Dielectric Spectroscopy*, Springer-Verlag Berlin Heidelberg, New York, (2003).

[41] M. Marzantowicz, J. R. Dygas, F. Krok, Z. Florjanczyk and E. Zygadlo-Monikowska, *J. Non-Crystalline Solids,* **352,** 5216 (2006).

[42] Srivastastava K K, Kumar A, Panwar O S and Lakshminarayan K N *J. Non-Cryst. Solids,* **33**, 205 (1979).

[43] El Anwar I M, Mohamad A K and Hammad F F *Egypt.J. Chem.,* **42**, 527–44 6 (1999).